Universality in adsorbate ordering on nanotube surfaces

V. I. Tokar[1,2] and H. Dreyssé[1]
[1]*IPCMS, Université de Strasbourg–CNRS, UMR 7504, 23 rue du Loess, F-67034 Strasbourg, France*
[2]*Institute of Magnetism, NAS and MES of Ukraine, 36-b Vernadsky Boulevard, 03142 Kiev-142, Ukraine*
(Received 24 January 2010; revised manuscript received 25 July 2010; published 27 September 2010)

Numerically efficient transfer-matrix technique for studying statistics of coherent adsorbates on small nanotubes has been developed. In the framework of a realistic microscopic model fitted to the data of *ab initio* calculations taken from literature sources, the ordering of potassium adsorbate on (6,0) single-walled carbon nanotube has been studied. Special attention has been paid to the phase transitionlike abrupt changes seen in the adsorption isotherms at low temperature. It has been found that the behavior during the transitions conforms with the universality hypothesis of the theory of critical phenomena and is qualitatively the same as in the one-dimensional Ising model. Quantitatively the critical behavior can be fully described by two parameters. Their qualitative connection with the properties of interphase boundaries is suggested but further research is needed to develop a quantitative theory.

DOI: 10.1103/PhysRevB.82.115446 PACS number(s): 64.70.Nd, 68.43.−h

I. INTRODUCTION

A considerable part of the ongoing research on adsorption in carbon nanostructures is driven by the problem of hydrogen storage at ambient conditions.[1–4] In particular, the metallic adsorbates are expected to considerably enhance the hydrogen uptake[2,4–7] because the storage capacity of purely carbon structures is insufficient from a practical point of view.[3] The adsorption of gases[8–11] allows, *inter alia*, to gain deeper insight into the dependence of sorption on various characteristics of adsorbate molecules, such as their size.[9]

From the storage perspective, the most promising among carbon nanostructures are the single-walled nanotubes (SWNTs) because of their large surface to weight ratio.[2,3] Since the storage capacity is defined mainly by the adsorbing surface,[3] theoretical studies of the adsorption for simplicity are often performed on individual SWNTs.[5–7,9,12] The hydrogen uptake predicted in such studies is sometimes very high[6,7,12] but their significance for the storage is not clear because the calculations are usually made for periodic structures at zero temperature with only crude estimates of temperature effects sometimes being made.[6,12]

Temperature effects, however, may strongly influence predictions based on zero-temperature calculations. For example, at finite temperatures the ordered structures cannot exist in one-dimensional (1D) systems in the thermodynamic limit.[13] Instead, if temperature is sufficiently low, a disordered state is formed with extended local order corresponding to the $T=0$ K ordered structure. From continuity considerations it is reasonable to assume that at sufficiently low temperature this quasiordered structure should be as good a hydrogen absorber as the zero-temperature one. Thus, from the storage point of view the question is how large are the temperatures at which the zero-temperature predictions can still be relied upon. In the closely related problem of adsorption on the two-dimensional (2D) surface this question can be answered with the help of phase diagrams where ordered and disordered phases are separated by well-defined boundaries.[14,15]

The aim of the present paper is to adopt the techniques of Refs. 14 and 15 where adsorption of hydrogen and oxygen on 2D surfaces were investigated to the case of adsorption on individual SWNTs and to find out what can be said about the quasiordered structures in the absence of well-defined finite-temperature phase boundaries. To implement this approach, some assumptions and approximations need be made which are usually specific to the type of the adsorbate under consideration. For concreteness, we will discuss them using as an example the potassium deposit on (6,0) zigzag SWNT. This choice was motivated mainly by the fact that this system was studied with an *ab initio* technique in Ref. 5 where the ground-state energies of six periodic structures were calculated. Such information is necessary for the implementation of the cluster expansion method (CEM) (Refs. 14 and 16–18) which allows one to derive an effective lattice-gas Hamiltonian to use in the solution of statistical problems. In connection with Refs. 16–18 which deal with binary alloys it is pertinent to point out that the lattice-gas model is formally equivalent to the binary alloy which allows for the use of techniques developed in the alloy theory to coherent surface adsorbates. It should also be noted that in nonmetallic systems the CEM can be developed on the basis of the energies calculated with the use of model potentials.[9] Furthermore, the effective Hamiltonian can be derived via fit to experimental data.[14,15]

An important assumption made in the application of CEM to surface structures is that the adsorbate is in registry with the substrate lattice. In reality, however, this depends on the relative strength of interactions of adsorbate atoms between themselves and with the substrate. If the latter interaction is weak (which is the case in the system under consideration[19]) the coherence with the substrate in sufficiently dense structures can be lost.[20]

Another difficulty is due to the substantial coverage-dependent charge transfer which strongly influences the interactions of adsorbate atoms with the substrate and with each other (see detailed discussion for the potassium deposits on graphite, graphene, and on SWNTs in Refs. 19 and 21). In principle, charge transfer should be adequately accounted for in the *ab initio* calculations.[5] But the system under consideration is apparently rather singular because the adsorption energy of potassium atom on the graphene varies in different

calculations from 0.44 to 2.0 eV.[21] On that scale our neglect of phonons whose characteristic Debye energy is usually an order of magnitude smaller looks justified. The question remains on the importance of the entropic contribution at finite temperature due to the atomic vibrations. In the case of alloys this problem was reviewed in Ref. 22 where it was concluded that in the majority of cases the classical approximation should be sufficient. At least, this is justifiable in the case of atoms with large atomic mass like potassium. The classical statistical averaging in the harmonic approximation on which the phonon theory is based reduces to the Gaussian integration over atomic coordinates which can be performed exactly. As explained in Appendix B of Ref. 23, the energy part of the configuration free energy thus obtained coincides with the energy minimum at zero temperature. Thus, the equilibrium atomic positions obtained in the *ab initio* calculations[5] at zero temperature provide the necessary average energy while the entropic part can be unified with the interaction part as an effective temperature-dependent contribution into the pair interatomic interaction.[22,23] Because in the present study we are going to consider temperatures which are small in comparison with the pair interactions, we will neglect this contribution in our calculations.

Finally, when deposited atoms or molecules are very light (He and H_2 being the most important examples), quantum corrections became important at low temperatures and quantum treatment is preferable.[24,25] In Ref. 24, however, it was shown for the hydrogen molecules adsorbed in the nanotube bundles that a fully classical regime sets in already at temperatures above 60 K. Because for the storage purposes the temperatures below the liquid nitrogen boiling point (77 K) are of little interest,[4] the quantum corrections can be neglected in the studies oriented on storage applications.

Thus, the main difficulties in the statistical description of the adlayers on SWNTs are due to the incommensurate structures and the poor accuracy of the interaction parameters. The accuracy can be improved either with the use of a better *ab initio* approach or by a direct fit to experimental data.[15] The loss of coherence with the substrate is a more serious problem because the lattice-gas formalism usually requires a regular lattice to exist (see, however, Sec. 5.3 of Ref. 18). In adsorbates this usually restricts the coverages at which the system retains its coherence to low values $\lesssim 0.5$.[8,19]

But on the other hand, as is well known (see, e.g., Ref. 17), the lattice-gas model is equivalent to the Ising model which is famous for being capable of describing such disparate critical phenomena as the magnetic ordering in uniaxial magnets and the liquid-gas phase transition.[26–28] This similarity between the critical phenomena has been conceptualized in the universality hypothesis which has been amply confirmed by both experimental data and theoretical calculations in 2D and three-dimensional (3D) systems.[29,30] Hopefully it will work equally well in 1D systems[31,32] which may allow for the extension of our results to the incommensurate cases as well.

In view of the many approximations and assumptions which need be accepted in order to implement the statistical approach to the adsorption on SWNTs, in the present paper we will focus on the low-temperature regions in the vicinity of critical points where the universal behavior sets in and where even significant inaccuracies in the microscopic description in most cases may be irrelevant.

In the next section we will explain the universality hypothesis for one-dimensional systems belonging to the Ising universality class; in Sec. III the effective Hamiltonian will be derived in the framework of the CEM; in Sec. IV the partition function will be calculated with the use of numerically efficient transfer-matrix (TM) technique; and in Sec. V we present our conclusions.

II. UNIVERSALITY IN 1D

Universality hypothesis constitutes one of pillars of the modern theory of critical phenomena.[29–31] It states that the singular part of the equations of state of all systems belonging to the same universality class has the same functional form in the vicinity of the critical point. Unique for each system are only two constant parameters which define the scales of variation in the (dimensionless) external field

$$L = h/k_B T \tag{1}$$

and of the reduced temperature

$$t \equiv (T - T_c)/T_c, \tag{2}$$

where T_c is the critical temperature. Thus, one may simplify the task of predicting the behavior of a system in the critical region by solving the simplest model belonging to the universality class of interest. The two parameters can be either found in independent calculations or derived from experimental data. For the general discussion of the universality we refer the interested reader to the vast literature on the subject[29–31] while below we will consider only the Ising universality class in 1D.[32–34] The peculiarity of this case is that there is no finite-temperature phase transitions in 1D. Therefore, the approach to universality based on scaling variables in Eqs. (1) and (2) cannot be applied straightforwardly because $T_c=0$ and the scaling variable t is undefined.

A solution to this problem was found in Ref. 32. It was noted that instead of the scaling parameter Eq. (2) the correlation length ξ can be used due to the relation

$$t \sim \xi^{-1/\nu}, \tag{3}$$

where ν is the critical index which defines the divergence of the correlation length as $\xi \sim t^{-\nu}$. Taking into account that in 1D all critical indices are known exactly, on the basis of Eqs. (3.40) and (3.41) of Ref. 32 the equation of state in the scaling region can be written as

$$M \approx W(L\xi/2), \tag{4}$$

where M is the magnetization normalized as

$$M(\pm\infty) = \pm 1 \tag{5}$$

and W is the scaling function. The latter is universal for all systems belonging to the Ising universality class in 1D except for two constant factors: one factor multiplying W thus changing the range of variation in M in Eq. (5) and another one before its argument. We used this arbitrariness in Eq. (4) by dividing the argument by two in comparison with Ref. 32.

This definition is more appropriate to our purposes and according to Eq. (3) it does not change the scaling relations which are invariant under rescalings.

The above formalism can be easily refashioned to describe the lattice-gas model via the equivalence transformation

$$\sigma_i = 2n_i - 1, \tag{6}$$

where $\sigma_i = \pm 1$ is the Ising spin on site i and $n_i = 0,1$ the corresponding occupation number. From this identity it follows that

$$h\sigma_i = \mu n_i - \mu/2, \tag{7}$$

where $\mu = 2h$.

The coverage is defined as the lattice-gas density

$$\rho = \langle n_i \rangle, \tag{8}$$

where the angular brackets denote statistical averaging and the dependence of ρ on the lattice site is absent because the system is assumed to be homogeneous and the spontaneous symmetry breaking is absent in 1D.[13]

According to Eqs. (6) and (7), Eq. (4) takes the form

$$(\rho - \rho_c)/(\Delta\rho/2) \approx W[(\mu - \mu_c)\xi/k_B T], \tag{9}$$

where μ_c is the chemical potential at the critical point and $\Delta\rho = \rho_+ - \rho_-$ is the total change in the density during the transition. Because at the critical point the critical density $\rho_c \approx (\rho_+ + \rho_-)/2$, the left-hand side of Eq. (9) varies in the same range as in Eq. (5). We note that to achieve this we had to divide $\rho - \rho_c$ on the right-hand side of Eq. (9) by $\Delta\rho/2$, not by ρ_c as suggested in Ref. 29. In this way we fix one of the arbitrary scale factors in our problem.

Thus, according to the universality principle the behavior of the system near any critical point can be describe with the use of only two constant scale factors provided the universal function W is known. The latter can be calculated for the simplest possible model, the Ising model with the first-neighbor interactions being the most obvious choice.

1D lattice-gas model

Exact solutions of the 1D Ising model can be found in many places, for example, in Eq. (3.39) of Ref. 32 or in Ref. 34. But below for completeness we present the solution of the equivalent lattice-gas model with the use of a variant of the nonsymmetric transfer-matrix technique[35,36] which in Sec. IV will be generalized to the case of nanotubes.

In the process of adsorption the number of atoms on the surface is governed by the chemical potential μ which may be controlled by the gas pressure if the adsorption from gaseous phase takes place (see, e.g., Ref. 12) or by the concentration of the adsorbate in the solution in the case of adsorption from a liquid. Therefore, the natural choice is the grand ensemble formalism with the partition function

$$\Xi = \operatorname*{Tr}_{n_i=0,1} e^{-\beta H}, \tag{10}$$

where $\beta = 1/k_B T$ and H the Hamiltonian; for brevity the term with the chemical potential $-\mu\Sigma_i n_i$ is considered to be included into H.[15] With the use of Eq. (10) the coverage can be found as [cf. Eq. (8)]

$$\rho = (\beta N)^{-1} d \ln \Xi / d\mu, \tag{11}$$

where N is the number of deposition sites. In the case of 1D lattice gas with only nearest-neighbor interaction V_1 (which we assume to be attractive) Eq. (10) can be written as

$$\Xi_{1D} = \operatorname*{Tr}_{n_j=0,1} e^{\beta\mu n_N} \prod_{i=1}^{N-1} \exp(\beta\mu n_i - \beta V_1 n_i n_{i+1}). \tag{12}$$

We assume free boundary conditions corresponding to nanotubes with open ends. According to Eq. (12), Ξ_{1D} can be calculated via the $N-$first power of the transfer matrix

$$\hat{T} = \begin{pmatrix} 1 & 1 \\ e^{\beta\mu} & e^{\beta(\mu - V_1)} \end{pmatrix}. \tag{13}$$

In the thermodynamic limit the reduced free energy Eq. (29) of the 1D lattice gas is

$$\phi_{1D} = -\beta^{-1} \ln \lambda_+, \tag{14}$$

where λ_+ is the largest eigenvalue of $\hat{T}$. The logarithm in Eq. (14) can be cast into the form

$$\ln \lambda_+ = \delta + \ln(\cosh \delta + \sqrt{\sinh^2 \delta + e^{\beta V_1}}), \tag{15}$$

where

$$\delta = \beta(\mu - V_1)/2 \equiv \beta(\mu - \mu_c)/2. \tag{16}$$

The coverage can be found as

$$\rho = \beta^{-1} d \ln \lambda_+ / d\mu = \frac{1}{2} + \frac{1}{2} \frac{\sinh \delta}{\sqrt{\sinh^2 \delta + e^{\beta V_1}}}. \tag{17}$$

As is easy to see, at low temperature $e^{\beta V_1} \to 0$ and $\rho(\delta)$ tends to the θ function. In other words, all variation in $\rho(\delta)$ is restricted to a narrow interval of $\mu \approx \mu_c$. That is why this region is so important. The interaction potential and the temperature may vary in very broad ranges but the values $\rho = 0$ to the left of the interval and $\rho = 1$ to the right of it will remain the same. In other words, these ranges of variation in μ do not provide much useful information on the microscopics of the system. In contrast, in the vicinity of μ_c the slope

$$\frac{d\rho}{d\mu} = \frac{\beta}{4} \frac{e^{\beta V_1} \cosh \delta}{(\sinh^2 \delta + e^{\beta V_1})^{3/2}} \tag{18}$$

will vary very strongly with temperature, with V_1, with μ, etc., so all quantities of interest are most easily measured near this quasitransition point.

At $\mu = \mu_c$ ρ in Eq. (17) is equal to 0.5. This means that both phases—$\rho = 0$ and $\rho = 1$—are present in the system in equal proportion. At low temperature according to Eqs. (18) and (31) the atoms are correlated at long distances so the system looks as an intermittent mixture of the pure phases separated by interphase boundaries (IPBs). In the model under consideration the boundary energy at $T = 0$ is easy to calculate. In the Ising spin representation Eqs. (6) and (7) the spin-spin interaction at $h = 0$ ($\rho = 0.5$) is

$$(V_1/4)\sum_i \sigma_i\sigma_{i+1} = V_1\sum_i n_i n_{i+1} - \mu N/2. \tag{19}$$

At zero temperature the IPB will separate the region of spins up from the spin-down region. According to Eq. (19), in comparison with the ordered system the energy cost is

$$E_b = |V_1|/2. \tag{20}$$

Furthermore, in a system with free boundaries there are two equally probable possibilities for an IPB: $\uparrow\downarrow$ and $\downarrow\uparrow$. Thus, there is the entropy $k_B \ln 2$ associated with the IPB.

In general case we may introduce the free energy of the IPB as

$$G_b = H_b - TS_b, \tag{21}$$

where H_b is the enthalpy of the boundary creation and S_b its entropy. The IPBs break long-range correlations between different parts of the system. Therefore, the correlations extend at the distances which are inversely proportional to the IPB concentration. The latter can be estimated as[13]

$$c_b = e^{-\beta G_b}. \tag{22}$$

As can be seen from the explicit 1D solution above, c_b also defines the width of the region around μ_c where the fast change in the adsorption isotherm takes place. This can be visualized with the use of the variable x introduced as

$$\beta(\mu - \mu_c) = c_b x. \tag{23}$$

With the use of this variable one can establish on the basis of Eq. (17) the explicit form of the universal function in Eqs. (4) and (9) as

$$W(x) \approx \frac{x}{\sqrt{1+x^2}}. \tag{24}$$

We note that $W(\pm\infty) = \pm 1$, as necessary. From practical point of view, Eqs. (9) and (17) are not very convenient for universality checks because both sides of these equations turn into zero at the critical point $\rho = \rho_c$. This means that in the data measured or calculated with finite precision on a nonsingular background the universal behavior can be obscured by the errors. The singular behavior can be considerably enhanced by differentiation with respect to the gas pressure (see Fig. 1 in Ref. 37) or with respect to the variable x

$$\frac{d\rho}{dx} = \frac{1}{2(1+x^2)^{3/2}}. \tag{25}$$

As will be shown in Sec. IV, this expression indeed describes the isothermal compressibility of coherent deposits on SWNTs near the steps of the adsorption isotherms.

III. MODEL

The configuration of a coherent deposit consisting of identical atoms or molecules in the submonolayer coverage regime can be fully characterized by the occupation numbers $n_i = 0, 1$ of the deposition sites $i = 1, N$. The configuration energy of the deposit can be expanded into an infinite series of effective cluster interactions (ECIs) as[14,16,17]

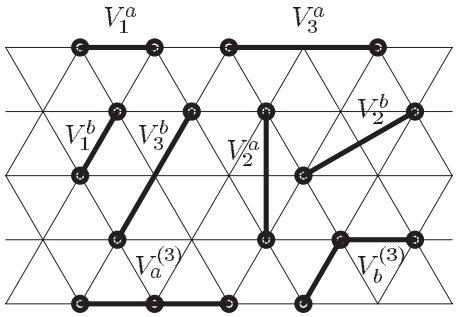

FIG. 1. Effective cluster interactions used to fit Hamiltonian in Eq. (26) to the *ab initio* data of Ref. 5. The triangular lattice of deposition sites is shown (the deposition site is defined as the center of the carbon hexagon, see Fig. 2). The tube axis is directed vertically. The leftmost and the rightmost sites in the odd rows on the drawing represent the same site on the tube.

$$H^{(N)} = (E_{ads} - \mu)\sum_i n_i + \sum_{i>j} V_{ij} n_i n_j + \sum_{i>j>k} V_{ijk}^{(3)} n_i n_j n_k + \cdots, \tag{26}$$

where we assumed that the system is homogeneous so the adsorption energy E_{ads} is the same at each site; also, as in Eq. (10), we included into the Hamiltonian the chemical potential μ to control the coverage. To find the interaction parameters in Eq. (26), one needs, according to established methodology,[14,16,17] to compute the energies of a sufficiently large number of different adsorbate structures and then fit these energies to the lattice-gas Hamiltonian (26) with sufficient number of ECIs. The energies are usually calculated *ab initio* but model calculations present viable alternative.[14,16,17] Yet another possibility is to adjust the interactions to the experimental data (see the discussion and the bibliography in Ref. 14).[38–41]

In our calculations below we consider the adsorption of potassium on the surface of the zigzag (6,0) carbon nanotube studied in Ref. 5 where the energies of six ordered structures were calculated within an *ab initio* approach. We remind that potassium and other metal deposits are directly related to the problem of hydrogen storage.[4–7,42]

From the structures considered in Ref. 5 one can deduce that at least third-neighbor pair interactions need be included into Hamiltonian (26) (see their Fig. 1 and our Figs. 1 and 2). Because of the tube anisotropy, the number of pair interac-

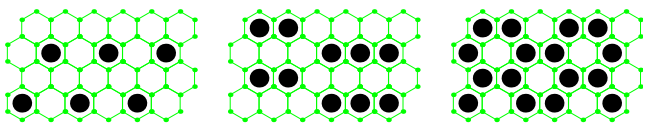

FIG. 2. (Color online) The ground-state structures on the surface of (6,0) SWNT with fillings 1/4, 5/12, and 2/3 found in Monte Carlo simulated annealing described in the text. The small dots correspond to the carbon atoms and the large dots the potassium atoms. The ranges of stability of these structures with the change in the chemical potential are shown in Fig. 3.

TABLE I. Interactions entering Hamiltonian in Eq. (26) (eV).

d	V_1^d	V_2^d	V_3^d	$V_d^{(3)}$	E_{ads}
a	−0.1072	-4.119×10^{-2}	-7.49×10^{-2}	0.242	−1.256
b	0.3427	−0.1084	−0.1268	-2.825×10^{-2}	

tions is, in fact, equal to six, as shown in Fig. 1. This is equal to the number of energy values we have at our disposition which is insufficient even to fit the pair interactions because we need also to determine the adsorption energy E_{ads}.

To overcome this difficulty we, following Ref. 43, assume that the pair interactions between the potassium atoms can be approximately described by the Morse potential

$$V(r_{ij}) = \epsilon(e^{-2a(r_{ij}-r_0)} - 2e^{-a(r_{ij}-r_0)}) \tag{27}$$

which depends on three parameters ϵ, a, and r_0. Taking into account E_{ads}, we are left with the possibility to adjust two more parameters. This turned out to be indispensable because the data of Ref. 5 could not be fitted to the Hamiltonian containing only pair interactions. This can be shown by expressing the energies of the structures in terms of (unknown) pair interactions and then establishing exact relations between some of the energies by excluding the pair interactions from the expressions. The sum rules obtained in this way are strongly violated by the data of Ref. 5.

Therefore, following Refs. 15 and 44–46 we added two trio interactions comprising closely spaced atoms.[17,46,47] By trial and error procedure we were able to achieve a very accurate fit to the six energies with two trio interactions shown in Fig. 1 and with the parameters presented in Table I.

The pair interactions presented in the table were obtained with the following parameters of the Morse potential: ϵ =0.136 eV, r_0=5.69 Å, and a=0.426. This can be compared with the values obtained for the adsorption of potassium on copper:[43] ϵ=0.466 eV, r_0=6 Å, and a=0.66. Taking into account that the systems are very different, our estimates look reasonable. A somewhat too small value of ϵ which define the attractive interaction between the potassium atoms may be due to the Coulomb repulsion because of the considerable and strongly coverage-dependent charge transfer between the potassium and the substrate.[19,21] The value of the adsorption energy in Table I also agrees well with recent *ab initio* estimates.[21]

Because our statistical approach is based on the grand ensemble, ECIs in Eq. (26) do not depend on the coverage ρ which does not enter as a parameter in the formalism but is a dependent quantity calculated according to Eq. (8). The concentration independence may look unphysical because the charge transfer which strongly influences the Coulomb interatomic interaction strongly depends on coverage.[19] Besides, in a similar problem in binary alloys it was shown that in the canonical formalism ECIs do depend on the concentration.[17,18] In Refs. 48 and 49, however, it was shown that, if properly implemented, both formalisms are equivalent. Formally in the grand ensemble the concentration-independent cluster interactions (the pair ones, the three-body, and higher) cooperate to reproduce the concentration dependence of the pair interactions of the canonical formalism.[48,49]

Physically the need for the three-body and higher ECIs can be understood as follows. In the case of only pair interactions there exists a "particle-hole" symmetry

$$H_{\text{pair}} = \sum_{i>j} V_{ij} n_i n_j - \mu \sum_i n_i = \sum_{i>j} V_{ij} \tilde{n}_i \tilde{n}_j - \mu' \sum_i \tilde{n}_i + C, \tag{28}$$

where $\tilde{n}_i \equiv 1-n_i$, μ' is a renormalized chemical potential, and C a configuration-independent constant. Because the chemical potential is an adjustable parameter fixing the coverage, in the case of constant pair interactions V_{ij} it follows from Eq. (28) that the free energies calculated for coverage ρ and $1-\rho$ differ only by the constant C. Thus, the derivatives of the free energy with respect to ρ whose singularities correspond to phase transitions (at least, in 2D and 3D systems) are distributed symmetrically with respect to $\rho=1/2$. This means that the phase diagram of the system with only pair interactions is strictly symmetric.[15] But physically this is rarely the case, so the presence of higher ECIs is very common. Quite often the asymmetry of the diagram is strong which require the presence of large three-body ECIs comparable in magnitude with the pair interactions.[15] As can be concluded from the value of the trio interaction $V_a^{(3)}$ in Table I, this is also the case in the potassium adsorbates under consideration.

IV. POTASSIUM ADSORPTION ON THE (6,0) SWNT

The model of potassium adsorption on the (6,0) SWNT considered in previous section can be solved with the use of the same TM technique as in Sec. II only the TM will be much more complex than Eq. (13). To account for all interactions shown in Fig. 1 we need the TM of a rather large size 2^{14}=16384, as explained in Appendix. Fortunately, only the largest eigenvalue is needed for our purposes so the efficient technique of finding extremal eigenvalues of nonsymmetric matrices due to Arnoldi as realized in the software package ARPACK (Ref. 50) could be used. Defining the reduced (per site) free energy

$$\phi = -\beta^{-1} \ln \Xi/N, \tag{29}$$

the coverage can be calculated as [see Eq. (11)]

$$\rho = \sum_i \langle n_i \rangle / N = -d\phi/d\mu. \tag{30}$$

The adsorption isotherms for three different temperatures shown in Fig. 4 were calculated according to this definition

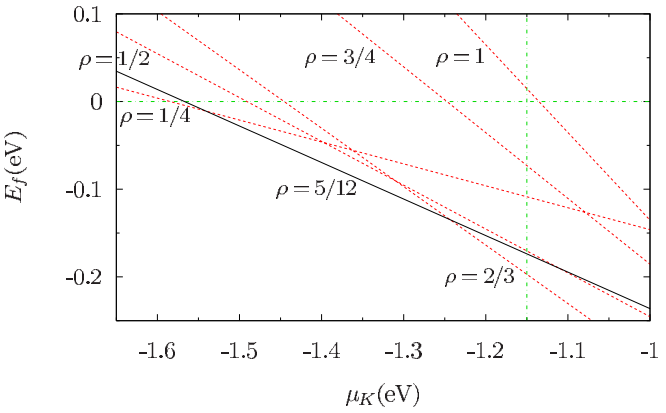

FIG. 3. (Color online) Zero-temperature phase diagram of potassium adsorbed on the surface of (6,0) carbon nanotube derived on the basis of Hamiltonian in Eq. (26) fitted to the data of Ref. 5. The dotted lines represent the fit to some of the structures found in that reference. The solid line corresponds to the new phase shown in Fig. 2. E_f is the energy of formation of the adsorbed structure and μ_K the chemical potential of potassium. The vertical line corresponds to bulk potassium (Ref. 5).

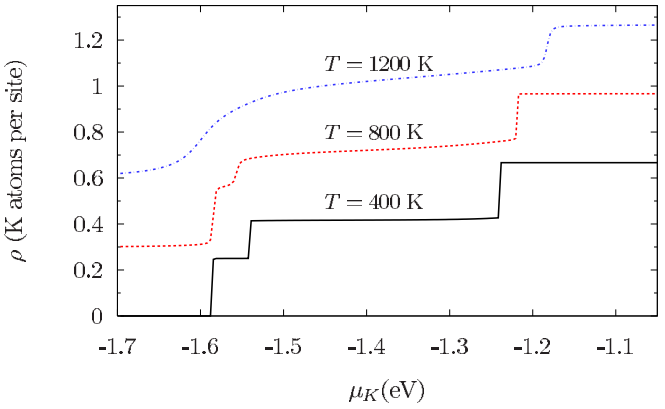

FIG. 4. (Color online) Adsorption isotherms at different temperatures for the system described by the Hamiltonian in Eq. (26) with parameters given in Table I. Upper curves are shifted up by 0.3 with respect to the preceding curve for better visibility.

with the use of the Hellmann-Feynman theorem to improve precision (see Appendix). As noted earlier, in the calculations we used Hamiltonian (26) with parameters from Table I. Though the parameters fitted the data of Ref. 5 very accurately, in our calculations we did not see the quasitransitions at or close to the values of the chemical potential shown in Fig. 2 of Ref. 5. Our TM solution, however, is exact up to the computational errors. Therefore, to establish the source of the discrepancy, we took the values of coverages at the lowest temperature (400 K) curve in Fig. 2 which to a high accuracy were equal to 1/4, 5/12, and 2/3 and performed Monte Carlo simulations in the framework of the canonical ensemble at these coverages.[51] The simulations with the use of the Metropolis algorithm were started at high temperatures and the system was gradually annealed to its ground state. At the coverages 1/4 and 2/3 we recovered the structures of Ref. 5 while at coverage 5/12 an additional structure shown in Fig. 2 was found. It turned out to have lower energy than their structure at $\rho=1/2$. This is shown in our Fig. 3 which is to be compared with Fig. 2(a) of Ref. 5.

From the point of view of the CEM, the appearance of a ground state unaccounted for in *ab initio* calculations diminishes the accuracy of the whole scheme because the ground states are the only ones directly observable in statistical calculations (as temperature tends to zero).[18] Therefore, it is highly desirable that they entered into the set of the structures calculated *ab initio*. While this point is important for the accuracy of the approach, in the present paper our main interest is in the universal features of the thermodynamics which do not depend on the accuracy of the Hamiltonian. So we believe that as long as the order of magnitude of the interactions are assessed correctly, the parameters of Table I are sufficiently adequate for our purposes.

Thus, according to our fit the $(2\times2)R0°$ structure from Fig. 2 is the ground state of Hamiltonian (26) in the interval of the chemical potentials $-1.585<\mu_K<-1.541$ eV (see Fig. 3), the 5/12 structure is stable for $-1.541<\mu_K<-1.243$ eV, and the $(\sqrt{3}\times\sqrt{3})R30°$ structure with $\rho=2/3$ is the energy minimum for μ_K larger than -1.243 eV and up to the chemical potential of the bulk potassium calculated in Ref. 5 to be equal to -1.15 eV (the vertical line in our Fig. 3). At finite temperature the zero-temperature boundaries between the ordered structures give rise to three quasitransition steps seen in Fig. 4. For simplicity we will refer to these transitions in order of their appearance from left to right as (quasi)transition number one, two, and three, respectively.

Isothermal susceptibility and the universality

The expression for the susceptibility with respect to the change in the chemical potential

$$d\rho/d\mu=\beta\sum_i\langle(n_i-\rho)(n_0-\rho)\rangle \tag{31}$$

can be derived form Eqs. (10) and (11). It can be used to assess the correlation length which we need in Eq. (9). As is known, both the susceptibility and the correlation length diverge at critical points.[26,31,32] Thus, the points of the quasiphase transitions in 1D at finite temperature can be identified as the maxima of the correlation length, as suggested in Ref. 52. Below we will determine in this way the value μ_c of the critical chemical potential. Besides, Eq. (31) can also be directly related to the isothermal compressibility because at constant temperature the chemical potential is proportional to the logarithm of the pressure of the ideal gas.[12] Furthermore, with the use of Eq. (7) this quantity can be directly connected with the magnetic susceptibility of the Ising model.

As can be seen from Fig. 4, the quasitransitions at the lowest temperature are so steep that can be easily confounded with the true first-order transitions. A possible check on whether the transition is the true one is via the susceptibility in Eq. (31) which should diverge at the true phase transition. We calculated this quantity by numerical differentiation of $\rho(\mu)$. The results are plotted in the form of Eq. (25) in Fig. 5. The parameters corresponding to the IPBs are presented in Table II. As can be seen, all values in the table are

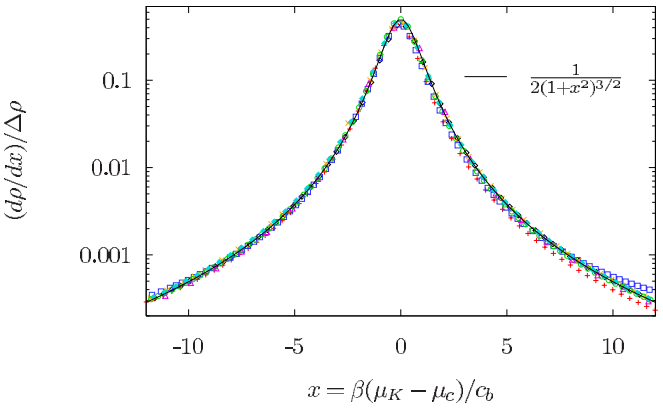

FIG. 5. (Color online) Low-temperature behavior of the susceptibility Eq. (31) during three quasitransitions seen in Fig. 4. The parameters defining c_b are presented in Table II. $\Delta\rho$ is the change in the coverage during the transition which is 1/4 in the first and the third transitions and 1/6 in the second one. The data plotted were calculated at temperatures $T=406$ K (♦), $T=464$ K (△), and $T=580$ K (○) near the first transition point, at $T=406$ K (×) and $T=580$ K (□) near the second transition point and at $T=464$ K (◇) and $T=580$ K (+) near the third-transition point.

reasonable from the point of view of the IPB interpretation: the entropies are all greater than the lower bound $k_B \ln 2 \approx 0.69 k_B$ of the purely 1D model of Sec. II and all enthalpies are notably larger than the individual interatomic interaction energies in Table I. We, however, were unable to calculate these values on the basis of an IPB model. Qualitatively it is clear that IPBs in our system correspond to the rearrangement of the atoms from one phase to another and taking into account the complexity of some of them (see our Fig. 2 and Ref. 5) the boundary may be not easy to guess. But even in the simplest case of the quasitransition 1 between the empty lattice and the $(2\times 2)R0°$ phase characterized by six third-neighbor couplings between the successive atomic layers (see Fig. 2), the naïve calculation $E_b=6V_3^b/2$ [by analogy with Eq. (20)] gives only 0.38 eV instead of 0.435. Also the entropy $2.4k_B$ suggests that the interface is rough, as is usual in 2D Ising-type systems.[53] In our Monte Carlo simulations, however, the IPBs were very flat, at least at low temperatures. Below we discuss some other possibilities which would require, however, additional investigations of this issue.

V. DISCUSSION

In the present paper with the use of numerically accurate technique we were able to resolve the very steep behavior seen in the isotherms of adsorption on the nanotube surfaces at low temperatures.[8] Such behavior is of considerable interest both from practical and from fundamental points of view. On the one hand, it describes the response of the system to small variations in the external parameters; on the other hand, the strong response to the changes in the parameters can provide accurate information about microscopic interactions.

TABLE II. Fitted values of the enthalpy and the entropy entering G_b in Eq. (21) for the three quasitransitions seen in Fig. 4.

Quasitransition No.	H_b (eV)	$S_b(k_B)$
1	0.435	2.40
2	0.545	4.34
3	0.420	0.80

In our calculations we used a realistic lattice-gas model containing six anisotropic pair interactions and two cluster interactions among atomic trios derived in the framework of the cluster expansion technique[14,16–18] on the basis of *ab initio* electronic-structure calculations.[5]

Despite the complexity of the model, its critical behavior turned out to be the same as in the 1D Ising (or, equivalently, lattice-gas) model with nearest-neighbor interactions. This agrees with the universality hypothesis of the theory of critical phenomena yet is a nontrivial result because contrary to 3D case,[29,30] in 1D this hypothesis cannot be justified in the framework of the renormalization-group approach for Hamiltonians with arbitrary interactions.[33] A qualitative explanation may be based on the very long-range correlations present in the system at low temperature. The correlation length which can be assessed from the right-hand side of Eq. (31) is of $O(1/c_b)$ and reaches values of $O(10^4)$ as can be estimated from Table II. This means that the structures are correlated at very long distances and, using the language of the renormalization group and the Ising model, the block spin transformation can be efficient in theoretical description of the system. Because the tube diameter is much smaller than the correlation length, the block spins will comprise all the spins around the tube circumference as well as considerable block of sites along the tube. In this picture the interactions of sufficiently short range will connect only the nearest-neighbor block spins thus making the system effectively equivalent to strictly 1D model with only nearest-neighbor interactions.

The correlation length in $O(10^4)$ of lattice spacings along the tube means that the whole nanotube can be covered by the ordered structure at temperatures as high as 400 K. (We note that only in infinite systems the long-range order should be broken in 1D;[13] in a finite system the order can extend along the whole tube length.[54]) Thus, from the hydrogen-storage standpoint, at ambient conditions the potassium structure can be treated as an inert (in statistical sense) substrate while the hydrogen molecules treated within a statistical approach which can be based on the formalism developed in the present paper.

In this study we concentrated on the universality for the following reasons. First, because we had at our disposition the energies of only six *ab initio* calculated structures, the accuracy of the cluster Hamiltonian was rather poor. Therefore, only orders of magnitude of the quantities of interest could be calculated judging from the fact that even 60 structures calculated in Ref. 14 did not allow to calculate the phase transition temperatures with accuracy better than 50%. The universal behavior, however, is the same for all Hamiltonians belonging to the same universality class. The second reason was that in many cases the surface structures are not commensurate with the substrate.[8,20] Yet they can be as good

hydrogen adsorbers as the commensurate structures. But, as we noted in the Sec. I, the lattice structure is not needed for the critical behavior to be universal, as the gas-liquid transitions in 1D, 2D, and 3D systems show.[26–28] According to Ref. 55 the liquid can be viewed as a crystalline state filled with topological defects, such as dislocations and disclinations. The same can be said about the incommensurate surface layers.[56] Therefore, one might expect that the universal critical behavior may take place also in the incommensurate cases. This prediction should be amenable to experimental verification on the isotherms of SWNTs covered with incommensurate phases of inert gases.[8]

The third reason for studying the universality was that while the TM technique is an accurate and efficient tool for treating the ordering of coherent adsorbates on surfaces of small nanotubes, the size of TM grows exponentially with the tube diameter and with the range of interactions. This means that for only slightly larger tube or longer-ranged interaction the TM will became unmanageably large. There exist viable alternatives to the TM in solution of this kind of problems: the mean-field approximation and especially the Monte Carlo method.[15,52,57,58] Both techniques, however, meet with difficulties in treating the fine details of the abrupt phase transitionlike changes seen on the adsorption isotherms. The results obtained in the present paper are aimed at resolving this difficulty. The mean-field or the Monte Carlo methods can accurately predict the position of the transition while the universality in the transition curves observed in our study should provide its fine details. There remains the problem of finding the values of the two parameters which describe the behavior quantitatively. A block-spin renormalization group and/or the low-temperature expansion are probable candidate tools for attacking this problem. Further work is needed to clarify this point.

ACKNOWLEDGMENTS

The authors acknowledge CNRS for support of their collaboration. One of the authors (V.I.T.) expresses his gratitude to Université de Strasbourg and IPCMS for their hospitality.

APPENDIX: SPARSE TRANSFER MATRICES

Our TM approach belongs to the general category of TM methods based on sparse matrices initiated in Refs. 35 and 36; further bibliography can be found in Ref. 59. The problem of adsorption on triangular lattice with account of the second-neighbor and trio interactions was previously studied within similar framework in Ref. 15 but no details were given. We believe that our technique presented below is particularly simple and easy to use.

The advantage of using sparse TMs is that instead of l^2 matrix elements of a conventional dense $l \times l$ TM matrix (see, e.g., Ref. 17) one deals with matrices containing only $O(l)$ nontrivial entries. Because the size of TM scales with the range of interactions R exponentially as

$$l = 2^R \tag{A1}$$

and in practical calculations reaches significant values (e.g., $2^{14}=16384$ in the present study), the gain in numerical efficiency from using sparse TMs can be enormous.

The interaction range R in Eq. (A1) for Hamiltonian (26) is defined as the longest range of the cluster interactions it contains. The range of a cluster interaction $V^{(m)}_{i_1 \cdots i_n} n_{i_1}, \ldots, n_{i_m}$ is defined as

$$R = i_{\max} - i_{\min}, \tag{A2}$$

where $i_{\max}$ and $i_{\min}$ are the maximal and the minimal indices among $i_1, \ldots, i_m$. For example, the cluster interaction $n_i n_{i+1} n_{i+2}$ has the range $R=2$.

The finite range of interactions in the Hamiltonian makes possible a recursive calculation of the partition function. This is because when adding a site to the system consisting of $K \geq R$ sites only the interactions with the last R sites need be taken into account. The accounting can be done with the use of the vector partition function $\vec{Z}^{(K)}$ whose components are the partial traces over all except the last R sites (the sites are numbered from right to left)

$$Z^{(K)}_{n_K, n_{K-1}, \ldots, n_{K-R+1}} = \mathrm{Tr}_{n_1, n_2, \ldots, n_{K-R}} \exp(-H^{(K)}), \tag{A3}$$

which can be visualized as

$$Z^{(K)}_{\underbrace{\bullet \circ \cdots \bullet}_{R}} = \overbrace{\bullet \circ \cdots \bullet}^{R} \overbrace{* * \cdots * *}^{K}, \tag{A4}$$

where the empty and filled circles correspond to the empty ($n_i=0$) or filled ($n_i=1$) sites in Eq. (A3) while asterisks denote the sites over which the trace over the two possible values of filling has been taken; $H^{(K)}$ is Hamiltonian (26) for a K-site system. The partition function is found from Eq. (A3) as

$$Z^{(K)} = \sum_{\bar{\alpha}=\bar{0}}^{\overline{2^R-1}} Z^{(K)}_{\bar{\alpha}}. \tag{A5}$$

Here the bar over the number denotes that its binary representation is meant

$$\bar{A} = (a_{R-1}, \ldots, a_1 a_0)_R, \tag{A6}$$

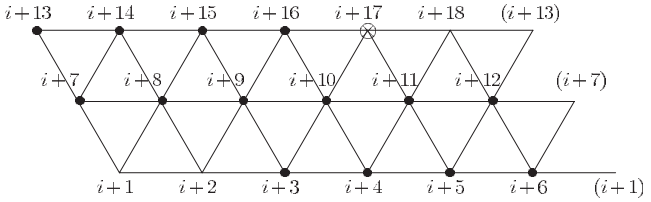

FIG. 6. Enumeration of sites on the (6,0) nanotube used in the construction of the TM. Black dots denote the 14 neighbors of site $i+17$. The 14th neighbor $i+3$ is defined by the interaction V^b_3 in Fig. 1.

where $a_k=0,1$ correspond to the filling of site k. The subscript R reminds that the term within parentheses is the binary representation, not the product, and that its length is equal to R. For example, $\bar{1}=00\ldots01$ with $R-1$ zeros before the unity means that there is $R-1$ empty sites before the filled one.

The general form of the TM can be understood from the recurrence equation

$$\begin{pmatrix} \circ\circ\ \ldots\ \circ\circ \\ \underbrace{\circ\circ\ \ldots\ \circ\bullet}_{R} \\ \vdots \\ \circ\bullet\ \ldots\ \bullet\bullet \\ \bullet\circ\ \ldots\ \circ\circ \\ \bullet\circ\ \ldots\ \circ\bullet \\ \vdots \\ \bullet\bullet\ \ldots\ \bullet\bullet \end{pmatrix}^{(N)} = \begin{pmatrix} 1 & 1 & 0 & 0 & \ldots & 0 & 0 & 0 \\ 0 & 0 & 1 & 1 & \ldots & 0 & 0 & 0 \\ \vdots & \vdots & \vdots & \vdots & \ddots & \vdots & \vdots & \vdots \\ 0 & 0 & 0 & 0 & \ldots & 0 & 1 & 1 \\ b_0 & b_1 & 0 & 0 & \ldots & 0 & 0 & 0 \\ 0 & 0 & b_2 & b_3 & \ldots & 0 & 0 & 0 \\ \vdots & \vdots & \vdots & \vdots & \ddots & \vdots & \vdots & \vdots \\ 0 & 0 & 0 & 0 & \ldots & 0 & b_{2^R-2} & b_{2^R-1} \end{pmatrix}^{(N)} \begin{pmatrix} \circ\circ\ \ldots\ \circ\circ \\ \underbrace{\circ\circ\ \ldots\ \circ\bullet}_{R} \\ \vdots \\ \circ\bullet\ \ldots\ \bullet\bullet \\ \bullet\circ\ \ldots\ \circ\circ \\ \bullet\circ\ \ldots\ \circ\bullet \\ \vdots \\ \bullet\bullet\ \ldots\ \bullet\bullet \end{pmatrix}^{(N-1)} \tag{A7}$$

where the column vectors correspond to $\vec{Z}^{(N-1)}$ and $\vec{Z}^{(N)}$ with the components denoted by their subscripts in Eq. (A4) for brevity. The subscript N of the TM is the site index for all $b_{\bar{\alpha}}$ entering the matrix. We note that we use the same symbol N for the system size and for the recurrent relation in order to stress that at every iteration we obtain the (vector) partition function of a system of size N, i.e., that the partition functions obtained at intermediary steps are not in any way deficient.

The structure of TM in Eq. (A7) is physically transparent. Having added site N to the system consisting of $N-1$ sites we first have to account for the interaction of this site with the rest of the system and then take the trace over the $(N-R)$th site because with the radius of interactions being R all interactions of this site with the rest of the system have already been taken into account. Taking the trace amounts to adding with appropriate weights two $Z^{(N-1)}$ differing by the filling of site $N-R$. In the case when site N is empty the weights are equal to unity because the empty site does not interact with anything and the interaction energy is zero. These terms occupy the upper half of the TM Eq. (A7). The lower half of the matrix contains the terms corresponding to the interaction of the *occupied* site N with the rest of the system. The term

$$b_{\bar{\alpha}N} = \exp(-\beta \Delta E_{\bar{\alpha}N}) \tag{A8}$$

is the Boltzmann weight corresponding to the interaction of the atom at site N with the configuration of atoms corresponding to $Z_{\bar{\alpha}}^{(N-1)}$; $\Delta E_{\bar{\alpha}N}$ in Eq. (A8) is the energy of interaction of the atom at site N with configuration $\bar{\alpha}$ on sites $N-1, N-2, \ldots, N-R$.

TABLE III. Interactions of atoms in the top row on Fig. 6 with atoms on 14 preceding sites (index i has been omitted for brevity). The arrows point to the value they represent.

Neighbor No.	13	14	15–16	17	18
1	V_1^b	V_1^a	←	←	←
2	V_2^b	←	V_3^a	←	←
4	0	←	←	V_3^a	←
5	V_2^b	←	←	←	V_1^a
6	V_1^b	←	←	←	←
7	V_2^a	V_1^b	←	←	←
8	V_3^b	←	V_2^b	←	←
11	0	←	←	←	V_2^b
12	V_3^b	←	←	←	←
13	0	V_2^a	←	←	←
14	0	←	V_3^b	←	←

1. Application to adsorption on (6,0) nanotube

In Fig. 6 are shown both the enumeration of sites we chose for the (6,0) nanotube and the 14 sites along the path with which atom at site $i+17$ can interact if they are also filled with atoms. The furthest neighbor site $i+3$ is defined by the third-neighbor interaction V_3^p which can reach it (see Fig. 1). Thus, according to Eq. (A2) $R=14$ and the size of our TMs is $2^{14}=16384$. This is the number of configurations we need to account for in our transfer matrices. From Fig. 6 one can see that as the sites are being added one after another in the top row the relative placement of the 14th neighbor change with respect to the added site. Because of this the transfer matrices for neighbor sites are different, except for sites $i+15$ and $i+16$ which is due to the particular interactions entering our Hamiltonian. This can be seen from Table III where the pair interactions accounted for in the Boltzmann factors b_k entering the TMs are presented. Similar tables can be composed for the trio interactions.

It is easy to see that the structure of the TMs repeats after each six steps, for example, when the row gets filled. This allows one to compute the reduced free energy of the system Eq. (14) through the logarithm of the largest eigenvalue λ_+ of the product of six TMs, e.g., of those corresponding to sites from $i+13$ to $i+18$ in Fig. 6 as

$$\phi = -k_B T \ln \lambda_+/6. \tag{A9}$$

2. Adsorption isotherms

To draw the adsorption isotherm one has to calculate the derivative of ϕ with respect to the chemical potential [see Eq. (30)]. With the fast variation in the derivative in the most interesting region in the vicinity of the quasitransition, the numerical differentiation can be unreliable. More accurate results can be obtained with the use of the Hellmann-Feynman theorem

$$\rho = -\frac{d\phi}{d\mu} = \frac{1}{6}\frac{\langle + | d\hat{M}_6/d(\beta\mu) | + \rangle}{\langle + | \hat{M}_6 | + \rangle}, \tag{A10}$$

where $\hat{M}$ is the product of the six TMs, as explained above, $|+\rangle$ is the eigenvector corresponding to λ_+, and $\langle +|$ the eigenvector of the transposed matrix because our TMs are not symmetric. Due to the simplicity of our TMs the derivative in Eq. (A10) is very easy to calculate: the upper part of each of the six TMs entering $\hat{M}$ should simply be successively set to zero while the lower part remains the same because the differentiation does not change the exponential function $\exp(\beta\mu)$.

[1] A. C. Dillon, K. M. Jones, T. A. Bekkedahl, C. H. Kiang, D. S. Bethune, and M. J. Heben, Nature (London) **386**, 377 (1997).
[2] P. Bénard and R. Chahine, Scr. Mater. **56**, 803 (2007).
[3] S. Bianco, M. Giorcelli, S. Musso, M. Castellino, F. Agresti, A. Khandelwal, S. Lo Russo, M. Kumar, Y. Ando, and A. Tagliaferro, J. Nanosci. Nanotechnol. **9**, 6806 (2009).
[4] Y. Yürüm, A. Taralp, and T. N. Veziroglu, Int. J. Hydrogen Energy **34**, 3784 (2009).
[5] X. Yang and J. Ni, Phys. Rev. B **69**, 125419 (2004).
[6] T. Yildirim and S. Ciraci, Phys. Rev. Lett. **94**, 175501 (2005).
[7] X. Yang, R. Q. Zhang, and J. Ni, Phys. Rev. B **79**, 075431 (2009).
[8] Z. Wang, J. Wei, P. Morse, J. G. Dash, O. E. Vilches, and D. H. Cobden, Science **327**, 552 (2010).
[9] A. D. Lueking and M. W. Cole, Phys. Rev. B **75**, 195425 (2007).
[10] T. Ohba, T. Matsumura, K. Hata, M. Yumura, S. Iijima, H. Kanoh, and K. Kaneko, J. Phys. Chem. C **111**, 15660 (2007).
[11] J. Zhao, A. Buldum, J. Han, and J. P. Lu, Nanotechnology **13**, 195 (2002).
[12] X. Yang and J. Ni, Phys. Rev. B **74**, 195437 (2006).
[13] L. Landau and E. Lifshitz, *Statistical Physics* (Pergamon Press, London, 1969).
[14] M. Stöhr, R. Podloucky, and S. Müller, J. Phys.: Condens. Matter **21**, 134017 (2009).
[15] W. Kinzel, W. Selke, and K. Binder, Surf. Sci. **121**, 13 (1982).
[16] J. M. Sanchez, F. Ducastelle, and D. Gratias, Physica A **128**, 334 (1984).
[17] F. Ducastelle, *Order and Phase Stability in Alloys* (North-Holland, Amsterdam, 1991).
[18] S. Müller, J. Phys.: Condens. Matter **15**, R1429 (2003).
[19] M. Caragiu and S. Finberg, J. Phys.: Condens. Matter **17**, R995 (2005).
[20] A. Šiber, Phys. Rev. B **68**, 033406 (2003).
[21] A. Lugo-Solis and I. Vasiliev, Phys. Rev. B **76**, 235431 (2007).
[22] A. van de Walle and G. Ceder, Rev. Mod. Phys. **74**, 11 (2002).
[23] V. I. Tokar and H. Dreyssé, Phys. Rev. B **68**, 195419 (2003).
[24] M. M. Calbi and M. W. Cole, Phys. Rev. B **66**, 115413 (2002).
[25] A. Šiber, Phys. Rev. B **66**, 205406 (2002).
[26] E. Brézin, D. J. Wallace, and K. G. Wilson, Phys. Rev. Lett. **29**, 591 (1972).
[27] G. L. Jones, J. Stat. Phys. **44**, 237 (1986).
[28] A. D. Bruce and N. B. Wilding, Phys. Rev. Lett. **68**, 193 (1992).
[29] D. Stauffer, M. Ferer, and M. Wortis, Phys. Rev. Lett. **29**, 345 (1972).
[30] H. E. Stanley, Rev. Mod. Phys. **71**, S358 (1999).
[31] M. E. Fisher, Rev. Mod. Phys. **46**, 597 (1974).
[32] D. R. Nelson and M. E. Fisher, Ann. Phys. **91**, 226 (1975).
[33] R. E. Prange, Phys. Rev. A **9**, 1711 (1974).
[34] R. G. Priest, Phys. Rev. B **11**, 3461 (1975).
[35] H. A. Kramers and G. H. Wannier, Phys. Rev. **60**, 252 (1941).
[36] C. Domb, Proc. R. Soc. London, Ser. A **196**, 36 (1949).
[37] Z. Mursic, M. Y. M. Lee, D. E. Johnson, and J. Z. Larese, Rev. Sci. Instrum. **67**, 1886 (1996).
[38] X. Yang and J. Ni, Phys. Rev. B **67**, 195403 (2003).
[39] S. R. Sharma, S. F. O'Shea, and W. J. Meath, Phys. Rev. B **40**, 6356 (1989).
[40] L. W. Bruch and A. D. Novaco, Phys. Rev. B **77**, 125435 (2008).
[41] M. A. Amat, M. Arienti, V. A. Fonoberov, I. G. Kevrekidis, and D. Maroudas, J. Chem. Phys. **129**, 184106 (2008).
[42] P. Chen, X. Wu, J. Lin, and K. L. Tan, Science **285**, 91 (1999).

[43] L. Padilla-Campos and A. Toro-Labbé, J. Chem. Phys. **108**, 6458 (1998).
[44] C. Stampfl, H. J. Kreuzer, S. H. Payne, H. Pfnür, and M. Scheffler, Phys. Rev. Lett. **83**, 2993 (1999).
[45] K. A. Fichthorn and M. Scheffler, Phys. Rev. Lett. **84**, 5371 (2000).
[46] W. Luo and K. A. Fichthorn, Phys. Rev. B **72**, 115433 (2005).
[47] V. I. Tokar and I. V. Masanskiy, Fiz. Met. Metalloved. **64**, 1207 (1987).
[48] M. Asta, C. Wolverton, D. de Fontaine, and H. Dreyssé, Phys. Rev. B **44**, 4907 (1991).
[49] C. Wolverton, M. Asta, H. Dreyssé, and D. de Fontaine, Phys. Rev. B **44**, 4914 (1991).
[50] R. Lehoucq, K. Maschhoff, D. Sorensen, and C. Yang, 1996, http://www.caam.rice.edu/software/ARPACK/
[51] K. Binder, in *Monte Carlo Methods in Statistical Physics*, Topics in Current Physics Vol. 7, edited by K. Binder (Springer-Verlag, Heidelberg, 1986), p. 1.
[52] M. R. Swift, E. Cheng, M. W. Cole, and J. R. Banavar, Phys. Rev. B **48**, 3124 (1993).
[53] D. B. Abraham, Commun. Math. Phys. **49**, 35 (1976).
[54] J. M. Phillips and J. G. Dash, J. Stat. Phys. **120**, 721 (2005).
[55] N. Rivier and D. M. Duffy, J. Phys. C **15**, 2867 (1982).
[56] J. C. Hamilton, R. Stumpf, K. Bromann, M. Giovannini, K. Kern, and H. Brune, Phys. Rev. Lett. **82**, 4488 (1999).
[57] R. A. Trasca, M. M. Calbi, and M. W. Cole, Phys. Rev. E **65**, 061607 (2002).
[58] R. A. Trasca, M. M. Calbi, M. W. Cole, and J. L. Riccardo, Phys. Rev. E **69**, 011605 (2004).
[59] N. H. Fuchs and S. Gartenhaus, Phys. Rev. B **31**, 7261 (1985).